Energy & Environmental Science

PAPER

View Article Online
View Journal | View Issue

Cite this: *Energy Environ. Sci.*, 2019, **12**, 2733

Redefining the Robeson upper bounds for CO_2/CH_4 and CO_2/N_2 separations using a series of ultrapermeable benzotriptycene-based polymers of intrinsic microporosity†

Bibiana Comesaña-Gándara, ‡[a] Jie Chen,‡[a] C. Grazia Bezzu, [a] Mariolino Carta, [b] Ian Rose,[a] Maria-Chiara Ferrari,[c] Elisa Esposito, [d] Alessio Fuoco, [d] Johannes C. Jansen *[d] and Neil B. McKeown *[a]

Membranes composed of Polymers of Intrinsic Microporosity (PIMs) have the potential for energy efficient industrial gas separations. Here we report the synthesis and gas permeability data of a series of ultrapermeable PIMs, of two-dimensional chain conformation and based on benzotriptycene structural units, that demonstrate remarkable ideal selectivity for most gas pairs of importance. In particular, the CO_2 ultrapermeability and high selectivity for CO_2 over CH_4, of key importance for the upgrading of natural gas and biogas, and for CO_2 over N_2, of importance for cost-effective carbon capture from power plants, exceed the performance of the current state-of-the-art polymers. All of the gas permeability data from this series of benzotriptycene-based PIMs are placed well above the current 2008 Robeson upper bounds for CO_2/CH_4 and CO_2/N_2. Indeed, the data for some of these polymers fall into a linear correlation on the benchmark Robeson plots [*i.e.* $\log(P_{CO_2}/P_{CH_4})$ *versus* $\log P_{CO_2}$ and $\log(P_{CO_2}/P_{N_2})$ *versus* $\log P_{CO_2}$], which are parallel to, but significantly above, that of the 2008 CO_2/CH_4 and CO_2/N_2 upper bounds, allowing their revision. The redefinition of these upper bounds sets new aspirational targets for polymer chemists to aim for and will result in more attractive parametric estimates of energy and cost efficiencies for carbon capture and natural/bio gas upgrading using state-of-the-art CO_2 separation membranes.

Received 29th April 2019,
Accepted 11th July 2019

DOI: 10.1039/c9ee01384a

rsc.li/ees

Broader context

The low-cost and energy-effective removal of carbon dioxide (CO_2) from natural gas and biogas would help the supply of methane as the cleanest burning and lowest carbon-emitting hydrocarbon fuel. In addition, carbon capture and storage (CCS) from power plant emissions will be required to achieve the goals of the 2015 Paris Agreement, which aspires to maintain global warming to less than 1.5 °C above that of the pre-industrial age by the end of the 21st Century. Indeed, the combined use of biofuels, such as biogas, and CCS technology is regarded as the key negative emissions technology required in order to reach the Agreement's ambitious targets for reduced emissions. Despite the urgent need for CCS, the best technology platform for its delivery is still unclear due to the difficulties in the estimation of costs and the complex evaluation of the advantages and disadvantages associated with each technology. Highly permeable membranes that are selective for CO_2 over methane (CO_2/CH_4) and CO_2 over nitrogen (CO_2/N_2) are of increasing interest for natural gas/biogas upgrading and carbon capture, respectively, due to the inherent efficiency of membrane separations. Here we report the synthesis of a series of ultrapermeable polymers that define the state-of-the-art in the trade-off between permeability and selectivity for all important gas separations and, in particular, for CO_2/CH_4 and CO_2/N_2. The data from these polymers were used to redefine the benchmark Robeson upper bounds for these two gas separations at much higher values of selectivity. This enhancement will improve the credibility of polymer membranes for CO_2 separations when evaluated against competing processes. Hopefully, this will help to stimulate the fundamental polymer science and applied engineering required to develop membrane systems for these CO_2 separations of key importance to energy and the environment.

Introduction

Membranes based on polymers as the selective layer are used for the energy efficient separation of gas mixtures including those of key relevance to energy and the environment.[1–4] The development of new polymers with greater gas permeability and selectivity would further enhance the efficiency of membrane gas separations of current industrial interest,[5] including hydrogen recovery during ammonia preparation (H_2 from N_2), oxygen or

[a] *EaStCHEM, School of Chemistry, University of Edinburgh, David Brewster Road, Edinburgh, EH9 3FJ, UK. E-mail: neil.mckeown@ed.ac.uk*
[b] *Department of Chemistry, Swansea University, College of Science, Grove Building, Singleton Park, Swansea, SA2 8PP, UK*
[c] *Institute for Materials and Processes, School of Engineering, The University of Edinburgh, Mayfield Road, Edinburgh EH9 3JL, UK*
[d] *Institute on Membrane Technology, ITM-CNR, Via P. Bucci 17/C, 87036 Rende (CS), Italy*

† Electronic supplementary information (ESI) available. See DOI: 10.1039/c9ee01384a

‡ The first two authors contributed equally.

nitrogen enrichment of air (O_2 from N_2)[6] and natural gas or biogas upgrading (predominantly CO_2 from CH_4).[7–10] Increasingly, polymer membranes are also being considered as a practical alternative to solvent absorption for large-scale capture of CO_2 from power plant flue gas (predominantly CO_2 from N_2).[7,9,11–14] For gas separations on such a massive scale, membranes with very high permeance (*i.e.* flux) are desirable to minimise energy costs for gas compression and to reduce the active surface area of the membrane, thereby, optimising the overall size and manufacture cost of the membrane system.[5,15] However, polymer membrane materials suffer from the well-established trade-off between gas permeability (P_x) and selectivity for one gas over another (P_x/P_y),[16,17] so that established ultrapermeable polymers, such as the polyacetylene poly(trimethylsilylpropyne) (PTMSP),[18,19] and recently reported examples[20] are insufficiently selective for use in gas separations.

The general trade-off between polymer permeability and selectivity was first quantified by Robeson in 1991 when he identified upper bounds in plots of $\log(P_x/P_y)$, *versus* $\log P_x$ for O_2/N_2, H_2/N_2, He/N_2, H_2/CH_4, He/CH_4, CO_2/CH_4, and He/H_2 gas pairs based on the gas permeability of the best performing polymers at that time.[21] Subsequently, for a newly prepared polymer (or a mixed matrix membrane)[22,23] the position of its gas permeability data relative to the upper bounds on Robeson plots allows for its potential for gas separations to be estimated. Robeson updated all of the upper bounds in 2008 using initial data for two spirobisindane-based Polymers of Intrinsic Microporosity (PIM-1 and PIM-7; Table S1, ESI†),[24] whose rigid and contorted macromolecular structures provided exceptionally high permeability with moderate selectivity.[25] In addition, data for these two PIMs were also used to define an upper bound for the CO_2/N_2 gas pair, which is of key importance to post-combustion carbon capture but had been considered of no practical interest in 1991.[24] Since 2008, many PIMs with enhanced rigidity have demonstrated gas permeability data that lie well above some of the 2008 upper bounds.[26] These highly shape-persistent PIMs were obtained by replacing the relatively flexible spirobisindane structural unit with spirobifluorene[27,28] units or highly rigid bridged bicyclic components such as ethanoanthracene,[29–32] triptycene,[33–36] methanopentacene[37] and Trögers base.[29,35] Indeed, in 2015 Pinnau *et al.*[38] proposed that the O_2/N_2, H_2/N_2 and H_2/CH_4 upper bounds should be updated using permeability data from aged films of highly selective triptycene-based PIMs (*e.g.* PIM-Trip-TB[35] and TPIM-1[33]). However, revisions of the upper bound for CO_2/N_2 and CO_2/CH_4 were not proposed at that time due to the data for these polymers and other high-performing PIMs being close to the existing 2008 CO_2/N_2 and CO_2/CH_4 upper bounds (Table S1, ESI†).

Recently, we introduced a new PIM derived from a benzotriptycene monomer, PIM-TMN-Trip, which proved to be as ultrapermeable to gases as PTMSP due to enhanced intrinsic microporosity arising from its 2D chain structure.[39] PIM-TMN-Trip demonstrates higher selectivity than PTMSP due to its greater chain rigidity providing enhanced molecular sieving (*i.e.* diffusivity selectivity). Furthermore, it was found that the unsubstituted benzotriptycene-based PIM (PIM-BTrip) demonstrates even greater selectivity placing its data above the proposed 2015 O_2/N_2, H_2/N_2 and H_2/CH_4 upper bounds and even above Robeson's 2008 upperbounds for CO_2/N_2 and CO_2/CH_4.[40,41] Here we report on the synthesis and properties of some new members of the benzotriptycene-based PIM series (Fig. 1), all of which demonstrate high permeability and selectivity. In particular, this polymer series demonstrates permeability data for CO_2/N_2 and CO_2/CH_4 that suggest new positions of the Robeson upper bound for these important gas pairs that are of key interest for separations of relevance to energy and the environment.

Results and discussion

Polymer design and synthesis

A further four benzotriptycene PIMs were synthesised along with new batches of PIM-TMN-Trip and PIM-BTrip to allow for direct comparison of their gas permeabilities. The novel polymers include PIM-HMI-Trip, for which the sterically crowded hexamethylindane (HMI)-solubilising group[42] would be expected to be more rigid than the tetramethylnaphthalene (TMN) group of PIM-TMN-Trip. Previously for spirobifluorene-based PIMs,[43] the introduction of adjacent methyl substituents had been

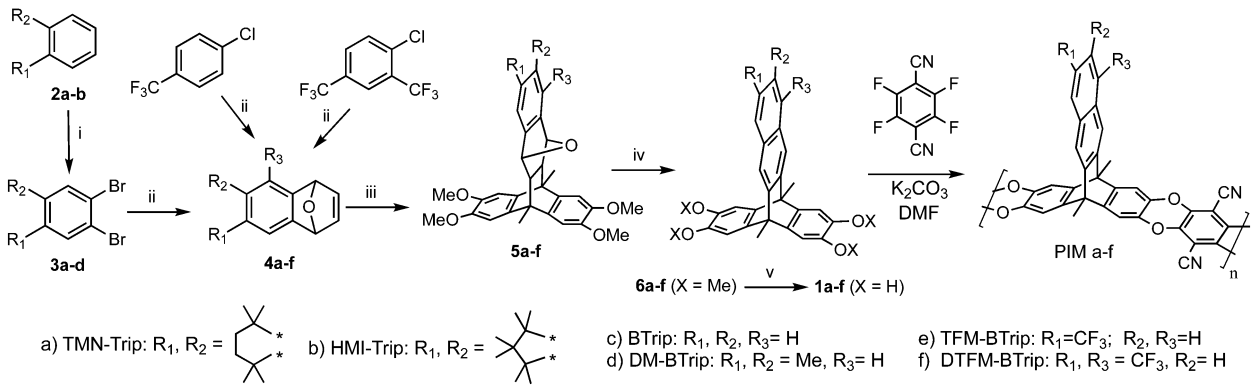

Fig. 1 Structure and synthesis of the benzotriptycene PIMs. Reagents and conditions: i. Br_2, Fe, DCM, rt, 3 h; ii. *n*-BuLi, furan, THF, −78 °C, 1.5 h; iii. 9,10-Dimethyl-2,3,6,7-tetramethoxyanthracene, DMF, 250 °C, 7 bar, 2 h, microwave irradiation, iv. TFA or $MeSO_4H$, rt, 24 h.; v. BBr_3, DCM. (See ESI† for details).

shown to be beneficial to performance, therefore, a PIM based on dimethylbenzotriptycene was prepared (PIM-DM-BTrip). In addition, the potential benefit of introducing one or two trifluoromethyl (TFM) solubilising groups onto the benzotriptycene unit was evaluated by the synthesis of PIM-TFM-BTrip and PIM-DTFM-BTrip, respectively.

Each polymer was prepared from its tetrahydroxy benzotriptycene monomer (**1a–f**) using the well-established benzodioxin-forming polymerisation reaction devised for PIM synthesis (Fig. 1).[44] Monomers were prepared by adaptation of the classic benzotriptycene synthesis, involving the Diels–Alder reaction between 2,3,6,7-tetramethoxy-9,10-dimethylanthracene and the appropriate 1,4-dihydro-1,4-epoxynaphthalene[39] – with the latter prepared from the Diels–Alder reaction between the appropriate benzyne intermediate and furan.[45–47]

PIM-TMN-Trip and PIM-HMI-Trip are both soluble in chloroform, facilitating analysis using Gel Permeation Chromatography (GPC) that confirmed that high molecular mass polymer was achieved for both polymers (Table 1). In contrast, PIM-DM-Btrip, PIM-TFM-BTrip and PIM-DTFM-BTrip proved soluble only in quinoline. The success of this high-boiling aromatic solvent for dissolving these otherwise intractable polymers prompted a re-investigation of the solubility of unsubstituted PIM-BTrip, which we had previously described as insoluble.[39] Pleasingly, this polymer also proved soluble in quinoline. Although quinoline is not an appropriate solvent for GPC analysis, solutions of PIM-DM-BTrip, PIM-TFM-BTrip, PIM-DTFM-BTrip and PIM-BTrip could be used to cast mechanically flexible and robust films, implying that a reasonably high molecular mass had been achieved during the synthesis. Synthetic and structural characterisation details, including solid state NMR (Fig. S1) are given in the ESI.†

Gas adsorption and gas transport properties.

In their powder form, all benzotriptycene-based PIMs adsorb a large amount of nitrogen (N_2, 77 K) at low relative pressure. Analysis of the N_2 adsorption isotherms (Fig. S1, ESI†) gives apparent Brunauer–Emmett–Teller (BET) surface areas (SA_{BET}) within the range of 848–1034 $m^2\ g^{-1}$ (Table 1), which are amongst the highest obtained from solution processable polymers.[29,39] The shapes of the N_2 isotherms are similar for all polymers except for PIM-TMN-Trip and PIM-DTFM-BTrip, for which there is larger uptake at higher pressures associated with a large hysteresis between the adsorption and desorption isotherms. This might be related to the TMN and CF_3 substituents protruding out of the 2D plane of the polymer chain and thus interfering with the electrostatic nitrile–nitrile interactions which are likely to dominate polymer cohesion. Adsorption of CO_2 at 273 K (Fig. S2, ESI†) shows similar uptakes for the benzotriptycene-PIMs (2.5–3.3 mmol g^{-1}). The uptake for PIM-BTrip is slightly higher at lower pressures, which may be ascribed to a greater concentration of ultramicropores (diameter < 0.7 nm in its pore size distribution (Fig. S3, ESI†)).

Solvent cast films (Fig. S4, ESI†) of the benzotriptycene-based PIMs all demonstrate exceptionally high gas permeability (Table 2). However, the evaluation of gas permeability data for a new polymer requires careful consideration of its film history and thickness as these factors influence greatly the observed values.[32] Generally, the highest reported values of gas permeability for high free volume polymers such as the PTMSP and PIMs were obtained from films freshly treated with methanol (or ethanol), which removes any residual casting solvent but also induces additional free volume.[31,48] The values of gas permeability from freshly methanol treated thick films (135–176 μm) of the benzotriptycene PIMs are some of highest reported for a pure polymer film (*e.g.*, $P_{CO_2} = 21–53 \times 10^3$ Barrer) and are comparable to those from ethanol treated ultrapermeable polyacetylenes (*e.g.*, $P_{CO_2} = 28–47 \times 10^3$ Barrer).[19,42] For each of the methanol treated films the order of decreasing gas permeability is $CO_2 > H_2 > O_2 > He > CH_4 > N_2$ with the exception of those from the less permeable and more size-selective PIM-BTrip for which He permeates faster than O_2. The ideal selectivities of all of the methanol treated films are significantly higher than those obtained for the ultrapermeable polyacetylenes and fall in the range of those reported for methanol treated films of less permeable PIMs such as PIM-1 (*e.g.*, $P_{O_2}/P_{N_2} = 2.6–3.6$).[48]

As noted for all PIMs and highly permeable polymers,[31,32,49–51] the extremely high values of gas permeability measured initially from the freshly methanol treated films are not maintained on ageing.[52] However, the reduction in permeability is accompanied by an increase in ideal selectivity for all gas pairs. In addition, on ageing, He permeability surpasses the value of O_2 for all the polymers, indicating enhanced size selectivity. Comparing data from approximately like-for-like samples (*i.e.* ~120 day aged and 110–180 μm thick films) the order

Table 1 Yield, molecular mass and gas adsorption properties of the benzotriptycene-based PIMs

Polymer	Yield (%)	Solubility	M_n (g mol^{-1})	M_w/M_n	η^a ($cm^3\ g^{-1}$)	$SA_{BET}{}^b$ ($m^2\ g^{-1}$)	$V_{Total}{}^c$ (ml g^{-1})	$V_M{}^d$ (ml g^{-1})	CO_2 uptake^e (mmol g^{-1})
PIM-TMN-Trip	67	$CHCl_3$	52 300^f	3.8	74	1034	0.87	0.38	3.3
PIM-HMI-Trip	58	$CHCl_3$	61 300^f	2.4	58	1033	0.71	0.38	3.0
PIM-BTrip	78	Quinoline	—^{g}	—^{g}	66	911	0.63	0.33	3.2
PIM-DM-BTrip	82	Quinoline	—^{g}	—^{g}	72	920	0.72	0.33	3.0
PIM-TFM-BTrip	79	Quinoline	—^{g}	—^{g}	37	848	0.66	0.31	2.5
PIM-DTFM-BTrip	84	Quinoline	—^{g}	—^{g}	65	964	1.02	0.33	2.5

^{a} Inherent viscosity in quinoline at 25 °C. ^{b} BET surface area calculated from N_2 adsorption isotherm obtained at 77 K. ^{c} Total pore volume estimated from N_2 uptake at $P/P_o = 0.98$. ^{d} Micropore volume estimated from N_2 uptake at $P/P_o = 0.05$. ^{e} CO_2 adsorption at 1 bar and 273 K. ^{f} Relative to polystyrene standards. ^{g} Not measured due to insolubility in solvents compatible with GPC analysis.

Table 2 Thickness (l, μm), ideal gas permeabilities (*P*x, Barrer) and selectivities of freshly methanol treated and aged films measured at 25 °C and 1 bar of feed pressure

PIM-[a]	l[b]	P_{N_2}	P_{O_2}	P_{CO_2}	P_{CH_4}	P_{H_2}	P_{He}	P_{O_2}/P_{N_2}	P_{H_2}/P_{N_2}	P_{CO_2}/P_{N_2}	P_{CO_2}/P_{CH_4}
BTrip	160	1190	4330	21 500	1690	12 100	4540	3.64	10.2	18.1	12.7
(130)[c,d]	160	522	2570	13 200	570	8440	3110	4.92	16.2	25.3	23.2
(253)[c,d]	160	401	2170	10 700	411	8930	3400	5.41	22.3	26.7	26.0
(365)[c,d]	160	280	1580	8020	282	7160	2810	5.65	25.6	28.6	28.4
(490)[c,d]	160	195	1240	6060	203	6380	2650	6.34	32.6	31.0	29.9
(633)[c,d]	160	127	935	4350	130	5100	2180	7.36	40.1	34.2	33.5
(718)[e,g]	160	112	838	3770	113	4820	2150	7.51	43.2	33.8	33.5
		(±4)	(±48)	(±166)	(±4)	(±186)	(±64)	(±0.19)	(±0.53)	(±0.53)	(±0.33)
BTrip[d]	64	339	1800	9200	412	9430	3960	5.31	27.8	27.1	22.3
(120)	64	200	1160	6040	237	7180	3020	5.79	35.8	30.2	25.5
(253)[d]	64	190	1143	5990	225	8080	3490	6.01	42.5	31.5	26.6
(371)[c,d]	64	154	997	5150	163	7730	3620	6.47	50.2	33.4	31.6
TMN-Trip	166	3540	10 400	52 800	7250	18 800	6490	2.94	5.31	14.9	7.28
(120)	166	1970	6620	33 300	3130	15 300	5600	3.36	7.77	16.9	10.6
(253)	166	1470	5440	25 900	2030	14 100	5190	3.71	9.59	17.6	12.8
(358)	166	1289	5082	23 648	1751	14 118	5290	3.94	11.0	18.4	13.5
(426)	166	1100	4620	20 400	1440	14 100	5420	4.20	12.8	18.5	14.2
HMI-Trip[d]	135	2560	8540	44 200	4870	16 600	5700	3.34	6.48	17.3	9.08
(1)[f,g]	135	2120	7380	39 000	3990	18 400	6500	3.49	8.95	18.6	9.94
		(±330)	(±989)	(±3680)	(±708)	(±1765)	(±762)	(±0.14)	(±2.16)	(±1.7)	(±1.44)
(120)	135	1440	5180	26 900	2150	11 800	4240	3.60	8.19	18.7	12.5
(253)	135	972	3930	18 900	1220	10 700	3960	4.04	11.0	19.5	15.6
(358)	135	907	3760	17 404	1083	11 141	4245	4.15	12.3	19.2	16.1
(426)	135	804	3580	16 400	967	11 000	4150	4.45	13.7	20.4	16.9
TFM-BTrip[c,d]	176	1830	6210	33 700	2280	13 600	5150	3.39	7.43	18.4	14.8
(123)[c]	176	1090	4230	22 100	1250	10 700	4120	3.88	9.82	20.3	17.7
(255)[c]	176	875	3640	18 400	953	9870	4050	4.15	11.3	21.0	19.3
(367)[c]	176	791	3450	17 000	873	10 100	4170	4.36	12.7	21.5	19.5
(496)	176	722	3260	15 600	792	9760	3920	4.51	13.5	21.6	19.7
DTFM-BTrip	112	3000	7770	42 600	4340	14 700	5860	2.59	4.90	14.2	9.82
(119)	112	1800	5410	29 000	2150	11 300	4690	3.01	6.28	16.1	13.5
(366)	112	1300	4460	22 900	1390	10 700	4590	3.41	8.23	17.5	16.4
(490)	112	864	3490	16 900	890	10 400	4770	4.04	12.1	19.6	19.0
(636)	112	741	3170	14 800	728	10 200	4730	4.27	13.8	20.0	20.3
DM-BTrip[d,f]	114	1020	3950	22 000	1570	11 400	4000	3.90	11.3	21.8	14.0
		(±133)	(±374)	(±1071)	(±85)	(±482)	(±354)	(±0.16)	(±1.07)	(±2.5)	(±1.5)
(128)[d]	114	521	2640	12 200	599	9870	3650	5.07	18.9	23.4	20.4

[a] Number in parentheses is the ageing time in days after methanol treatment. [b] Thickness did not exhibit significant changes upon ageing. [c] Data defining the proposed CO_2/CH_4 upper bound. [d] Data defining the proposed CO_2/N_2 upper bound. [e] Average and standard deviation (in parentheses) of four independent measurements of the same aged sample. [f] Average and standard deviation (in parentheses) of four independent samples. [g] Data not included on Robeson plots (Fig. 2).

of decreasing permeability and increasing selectivity for the benzotriptycene PIMs is PIM-TMN-Trip > PIM-DTFM-BTrip > PIM-HMI-Trip > PIM-TFM-Trip > PIM-BTrip ≈ PIM-DM-BTrip. It can be deduced that the bulky TMN and HMI substituents both enhance permeability greatly, with the more rigid HMI substituent providing slightly higher selectivity over TMN. The relatively small $-CF_3$ substituents of PIM-TFM-BTrip and PIM-DTFM-BTrip also enhance permeability relative to unsubstituted PIM-BTrip. Interestingly, the $-CF_3$ substituents appear to slow ageing, with 54% of the value for P_{O_2} of the methanol treated film of PIM-DTFM-BTrip retained after one year, and 56% for PIM-TFM-BTrip, as compared to only 30–36% for films without $-CF_3$ substituents.

Depending on the gas, the standard deviation of the permeability is in the range 4–18% for the freshly MeOH treated PIM-HMI-Trip and PIM-DM-BTrip films, and 3–6% for the aged PIM-BTrip film. These are small compared to the effect of the ageing in this work, and almost negligible when represented on the double-logarithmic Robeson diagrams (Fig. S6, ESI†).

A thinner film of PIM-BTrip (64 μm) demonstrates lower initial permeability after methanol treatment, consistent with the well-established trend that thinner films age more rapidly than thicker films.[32,52,53] It is also more size selective than the thicker film of the same polymer with $H_2 > CO_2 > He > O_2 > CH_4 > N_2$ the order of decreasing gas permeability. Due to the commonly encountered variability of gas permeability from differing film thicknesses and history, data for a new polymer are best compared to those of existing polymers by using Robeson plots (Fig. 2). As noted, the position of the data from a new polymer relative to the Robeson upper bounds provides a useful indicator of its potential performance as gas separation membranes. All data points for the benzotriptycene polymers lie far above the 2008 upper bounds for O_2/N_2 (Fig. 2a), H_2/N_2 (Fig. 2b), H_2/CH_4, CO_2/N_2 (Fig. 2c) and CO_2/CH_4 (Fig. 2d). Data for the ~1 year aged films for all of the polymers lie close to the proposed 2015 upper bound for O_2/N_2. In particular, aged PIM-BTrip demonstrates exceptional selectivity for a highly permeable polymer so that its data lie well above the proposed

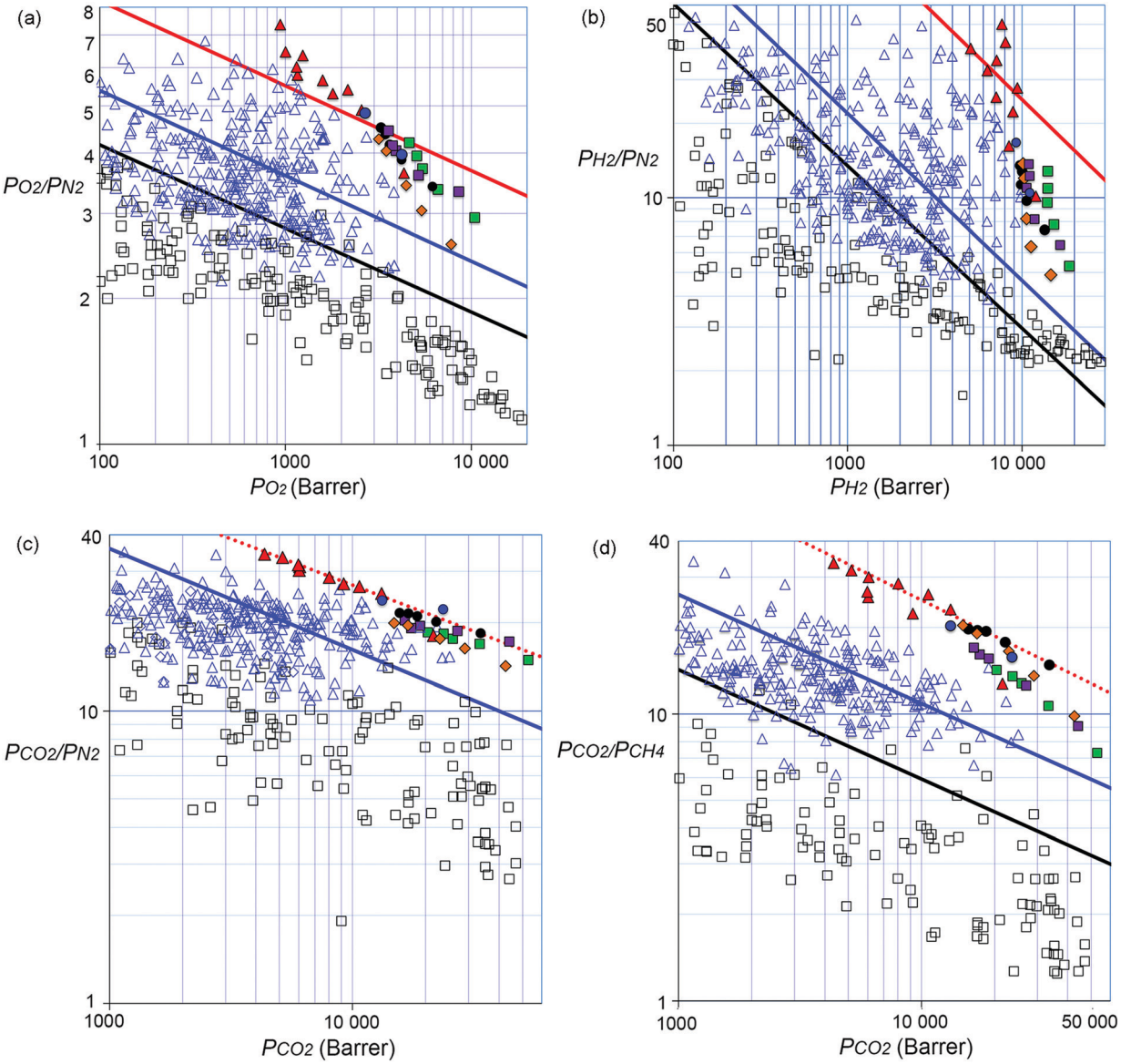

Fig. 2 Robeson plots for the (a) O_2/N_2, (b) H_2/N_2, (c) CO_2/N_2 and (d) CO_2/CH_4 gas pairs showing the position of the gas permeability data for films of PIM-BTrip (▲), PIM-TMN-Trip (■), PIM-HMI-Trip (■), PIM-DM-BTrip (●), PIM-TFM-BTrip (●) and PIM-DTFM-BTrip (◆). Previously reported data are also shown for non-PIM polymers (□) and PIMs (△). Upper bounds are represented by black lines (1991), blue lines (2008), and red lines for the previously proposed (2015) upper bounds for O_2/N_2 and H_2/N_2. The proposed revised upper bounds for CO_2/N_2 and CO_2/CH_4 are shown as dotted red lines.

2015 upper bounds for O_2/N_2 (Fig. 2a), H_2/N_2 (Fig. 2b), and H_2/CH_4. A notable feature of the permeability data from aged samples of the benzotriptycene-PIMs on the O_2/N_2 and H_2/N_2 Robeson plots is the near linear correlation at a steeper slope than that of the upper bounds (Fig. S5, ESI†). This reflects the far larger reduction of permeabilities on ageing for gases composed of larger molecules such as N_2 and CH_4 as compared to those composed of the smaller O_2 and H_2 molecules.

Gas transport through a polymer is described by the solution-diffusion model[54] with $P_x = D_x \times S_x$, where D_x is the diffusivity coefficient (Table S2, ESI†) and S_x is the solubility coefficient for gas x (Table S3, ESI†). Therefore, the ideal selectivity (P_x/P_y) for a polymer comes from a combination of diffusivity selectivity (D_x/D_y) and solubility selectivity (S_x/S_y). The remarkable positions of the data for the benzotriptycene-PIMs on the H_2/N_2, and O_2/N_2 Robeson plots are due to very high diffusivity selectivity originating from the size-sieving behaviour of the polymers, which differentiates between gas molecules of differing effective diameters (d_x).[40] This is best illustrated by the correlation between d_x^2 and the diffusivity coefficient (D_x),[55] which is steepest for PIM-BTrip and less steep for benzotriptycene PIMs that possess a substituent, although the absolute value of the diffusion coefficient is larger (Fig. 3). Ageing decreases the diffusion coefficient for all polymers but steepens the correlation between d_x^2 and D_x, especially for PIM-BTrip, which is evidence of its further enhanced size selectivity (Fig. S7, ESI†).[40] The extraordinary performance of PIM-BTrip can be attributed to its ultramicroporosity, which facilitates the diffusivity of small

gas molecules, together with very high chain rigidity,[16,54] which hinders the activated transport of larger gas molecules by reducing thermal motions that allow gaps to form between voids. The extreme rigidity of PIM-BTrip accounts for the very high activation energy for the diffusion of larger gases such as N_2 and CH_4.[40] The gas transport properties of PIM-BTrip appears similar to those reported for the two triptycene-derived polymers, PIM-Trip-TB[35] and TPIM-1,[33] which were used to define the proposed 2015 upper bounds for O_2/N_2, H_2/N_2 and H_2/CH_4.[38] It should be noted that the data from PIM-Trip-TB used to define the 2015 upper bounds were taken from a film that was aged for only 100 days after methanol treatment.[35] Recent remeasurement of the gas permeability of this film after 1900 days gives data that are also well over the proposed 2015 upper bounds for O_2/N_2 (*i.e.* P_{O_2} = 532 Barrer; P_{O_2}/P_{N_2} = 8.2) and H_2/N_2 (*i.e.* P_{H_2} = 4430 Barrer; P_{H_2}/P_{N_2} = 65). Therefore, the design concepts used to obtain the extraordinary size selectivity demonstrated by PIM-BTrip and PIM-Trip-TB are likely to provide PIMs that will provoke future significant revisions of the O_2/N_2, H_2/N_2 and H_2/CH_4 Robeson upper bounds.

Redefining the CO_2/N_2 and CO_2/CH_4 upper bounds

Separations involving CO_2 are mechanistically more complex than those governed predominately by diffusivity selectivity (*e.g.* O_2/N_2 or H_2/N_2) because S_{CO_2} dominates transport, especially for CO_2/N_2 due to the similar effective diameters of the two gas molecules. Typically for PIMs, values for S_{CO_2}/S_{N_2} lie in the range 15–20 whereas those for D_{CO_2}/D_{N_2} lie between 0.9–1.5 and these values are similar for PIMs with both higher and lower P_{CO_2} permeability. In general, solubility selectivity tends to remain fairly constant during ageing, in contrast to the increases observed for ideal selectivity values for transport dominated by diffusivity selectivity.[52] Thus, plotting data for previously reported PIMs on the Robeson plot for CO_2/N_2 shows many data points slightly above the 2008 upper bound at higher permeability (P_{CO_2} > 3000 Barrer) but few at lower values of permeability. Indeed, very few highly permeable polymers possess a CO_2/N_2 selectivity > 30,[56–59] which is the lower limit of interest for a first-pass polymer membrane for post-combustion carbon capture (Table S1, ESI†).[12]

Although all of the data for the benzotriptycene PIMs are above the 2008 upper bound for CO_2/N_2, the data from PIM-BTrip are particularly promising with both thick and thinner aged films providing P_{CO_2} > 4000 Barrer and P_{CO_2}/P_{N_2} > 30. The impressive performance of PIM-BTrip appears to be due to an unusually high D_{CO_2}/D_{N_2} of 2.0, whereas that of the substituted members of the series relies on greater S_{CO_2}/S_{N_2} resulting from the greater number of CO_2 adsorption sites provided by the larger amount of intrinsic microporosity (Table S3, ESI†). The eleven data points on the Robeson plot from four different polymers that fall into a linear correlation parallel to that of the 2008 upper bound allows us to propose a substantially improved new upper bound for CO_2/N_2 (Fig. 2c and Tables 2 and 3). These data points are distributed over a large P_{CO_2} range of 4400–52 000 Barrer.

In addition, the data for all of the benzotriptycene PIMs lie well above the 2008 upper bound for CO_2/CH_4 at a higher selectivity than those of previously reported polymers. Indeed, only data for the highly rigid "intermolecularly-locked" derivative of PIM-1 (PIM-C1)[60] and PIM-SBF-2[43] come close to those of the benzotriptycene PIMs (Table S1, ESI†). This exceptional performance appears due to a combination of both high diffusivity selectivity, with D_{CO_2}/D_{CH_4} in the range 5.7–9.5 for aged films, and good solubility selectivity (S_{CO_2}/S_{CH_4} > 3). Ten data points from two different polymers allows us to propose a new upper bound for CO_2/CH_4 parallel to that of 2008 (Fig. 2d and Tables 2 and 3). The benzotriptycene PIMs that either define or provide data that are very close to this revised upper bound are either unsubstituted (PIM-BTrip) or possess only small substituents (*i.e.* PIM-DM-BTrip; PIM-TFM-BTrip and PIM-DTFM-BTrip). In contrast, those possessing larger cyclic solubilising groups (*i.e.* PIM-TMN-Trip and PIM-HMI-Trip) are slightly less selective.

When defining his 2008 CO_2/CH_4 upper bound, Robeson noted that data for a series of Thermally Rearranged (TR)

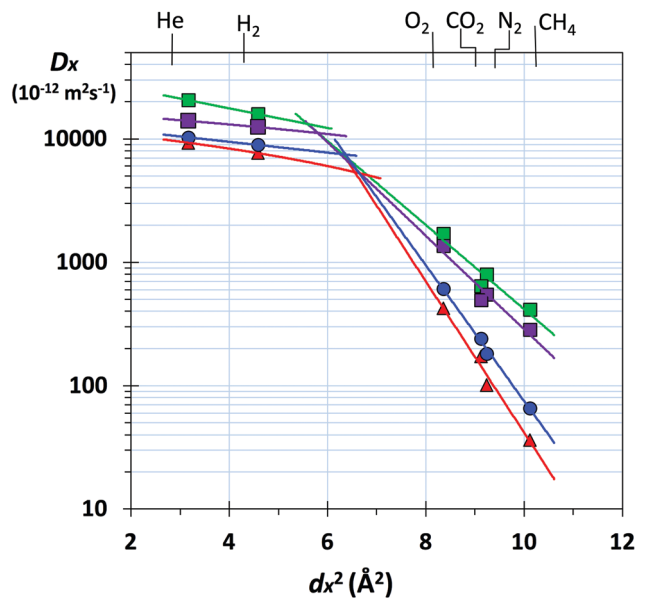

Fig. 3 Plot of diffusivity coefficient (D_x) *versus* d_x^2 (where d_x = effective diameter of gas molecule x: He = 1.78; H_2 = 2.14; O_2 = 2.89; CO_2 = 3.02; N_2 = 3.04; CH_4 = 3.18 Å)[55] for freshly methanol treated films of PIM-BTrip (▲), PIM-TMN-Trip (■), PIM-HMI-Trip (■), PIM-DM-BTrip (●). Data for PIM-TFM-BTrip and PIM-DTFM-BTrip are not shown for clarity but are very similar to those for PIM-TMN-Trip and PIM-HMI-Trip, respectively.

Table 3 Fitting parameters for the 2008 and proposed CO_2/N_2 and CO_2/CH_4 upper bounds using the formula $P_x = k\alpha_{xy}^n$ (where P_x is permeability (Barrer) of the most permeable x-gas, k is the front factor (Barrer), α_{xy} is the selectivity for x/y gas pair, and n is the slope)

	k (Barrer)	n
Robeson 2008 upper bounds[24]		
CO_2/CH_4	5.369×10^6	−2.636
CO_2/N_2	30.967×10^6	−2.888
Proposed upper bounds		
CO_2/CH_4	22.584×10^6	−2.401
CO_2/N_2	755.58×10^6	−3.409

polymers, reported by Park *et al.*,[15,61] "with exceptional CO_2/CH_4 separation capabilities",[24] appeared to form an upper bound above that proposed for solution processable polymers. Such insoluble network polymers as the TR polymers often perform above the 2008 upper bounds defined for solution processable polymers due to their rigidity approaching that of carbon molecular sieves (*i.e.* polymers carbonised at high temperatures). Remarkably, the CO_2/CH_4 upper bound defined by the solution processable benzotriptycene-based PIMs lies at the same position as that of Robeson's tentatively proposed TR polymer upper bound with a selectivity 2.5 times higher than that for the 2008 upper bound.

Conclusions

The benzotriptycene-based PIMs provide exceptional gas permeability data for most important gas pairs and allow for the redefinition of the CO_2/CH_4 and CO_2/N_2 Robeson upper bounds. This is important in order to set aspirational targets for chemists in the design and synthesis of novel polymers. In addition, it will help parametric studies of energy and cost efficiency for carbon capture and natural/bio gas upgrading by providing enhanced but realistic state-of-the-art values for membrane permeability and selectivity. The resulting estimates of energy efficiencies and costs will be more attractive relative to both previous calculations for membrane systems and to competitive CO_2 separation processes. The resulting improved credibility of polymer membranes for these crucial separations will stimulate research activity in this technological area of prime importance to energy and the environment.

Conflicts of interest

There are no conflicts of interest to declare.

Acknowledgements

The research leading to these results has received funding from the EU FP7 Framework Program under grant agreement no. 608490, project M^4CO_2 and from the EPSRC (UK) grant numbers EP/M01486X/1, EP/R000468/1 and EP/K008102/2.

References

1 P. Bernardo, E. Drioli and G. Golemme, *Ind. Eng. Chem. Res.*, 2009, **48**, 4638–4663.
2 Y. Yampolskii, *Macromolecules*, 2012, **45**, 3298–3311.
3 R. W. Baker and B. T. Low, *Macromolecules*, 2014, **47**, 6999–7013.
4 M. Galizia, W. S. Chi, Z. P. Smith, T. C. Merkel, R. W. Baker and B. D. Freeman, *Macromolecules*, 2017, **50**, 7809–7843.
5 P. M. Budd and N. B. McKeown, *Polym. Chem.*, 2010, **1**, 63–68.
6 R. S. Murali, T. Sankarshana and S. Sridhar, *Sep. Purif. Rev.*, 2013, **42**, 130–186.
7 S. F. Wang, X. Q. Li, H. Wu, Z. Z. Tian, Q. P. Xin, G. W. He, D. D. Peng, S. L. Chen, Y. Yin, Z. Y. Jiang and M. D. Guiver, *Energy Environ. Sci.*, 2016, **9**, 1863–1890.
8 J. K. Adewole and A. L. Ahmad, *J. Polym. Res.*, 2017, **24**, 17.
9 N. Y. Du, H. B. Park, M. M. Dal-Cin and M. D. Guiver, *Energy Environ. Sci.*, 2012, **5**, 7306–7322.
10 E. Esposito, L. Dellamuzia, U. Moretti, A. Fuoco, L. Giorno and J. C. Jansen, *Energy Environ. Sci.*, 2019, **12**, 281–289.
11 M. C. Ferrari, D. Bocciardo and S. Brandani, *Green Energy Environ.*, 2016, **1**, 211–221.
12 T. C. Merkel, H. Q. Lin, X. T. Wei and R. Baker, *J. Membr. Sci.*, 2010, **359**, 126–139.
13 R. W. Baker, B. Freeman, J. Kniep, X. T. Wei and T. Merkel, *Int. J. Greenhouse Gas Control*, 2017, **66**, 35–47.
14 L. S. White, K. D. Amo, T. Wu and T. C. Merkel, *J. Membr. Sci.*, 2017, **542**, 217–225.
15 S. Kim and Y. M. Lee, *Prog. Polym. Sci.*, 2015, **43**, 1–32.
16 B. D. Freeman, *Macromolecules*, 1999, **32**, 375–380.
17 H. B. Park, J. Kamcev, L. M. Robeson, M. Elimelech and B. D. Freeman, *Science*, 2017, **356**, eaab0530.
18 T. Masuda, E. Isobe, T. Higashimura and K. Takada, *J. Am. Chem. Soc.*, 1983, **105**, 7473–7474.
19 Y. Yampolskii, *Polym. Rev.*, 2017, **57**, 200–212.
20 Y. He, F. M. Benedetti, S. Lin, C. Liu, Y. Zhao, H.-Z. Ye, T. Van Voorhis, M. G. De Angelis, T. M. Swager and Z. P. Smith, *Adv. Mater.*, 2019, **31**, 1807871.
21 L. M. Robeson, *J. Membr. Sci.*, 1991, **62**, 165–186.
22 S. Budhathoki, O. Ajayi, J. A. Steckel and C. E. Wilmer, *Energy Environ. Sci.*, 2019, **12**, 1255–1264.
23 C. Y. Chuah, K. Goh, Y. Q. Yang, H. Q. Gong, W. Li, H. E. Karahan, M. D. Guiver, R. Wang and T. H. Bae, *Chem. Rev.*, 2018, **118**, 8655–8769.
24 L. M. Robeson, *J. Membr. Sci.*, 2008, **320**, 390–400.
25 P. M. Budd, K. J. Msayib, C. E. Tattershall, B. S. Ghanem, K. J. Reynolds, N. B. McKeown and D. Fritsch, *J. Membr. Sci.*, 2005, **251**, 263–269.
26 M. D. Guiver and Y. M. Lee, *Science*, 2013, **339**, 284–285.
27 X. Ma, O. Salinas, E. Litwiller and I. Pinnau, *Macromolecules*, 2013, **46**, 9618–9624.
28 X. Ma, B. Ghanem, O. Salines, E. Litwiller and I. Pinnau, *ACS Macro Lett.*, 2015, **4**, 231–235.
29 M. Carta, R. Malpass-Evans, M. Croad, Y. Rogan, J. C. Jansen, P. Bernardo, F. Bazzarelli and N. B. McKeown, *Science*, 2013, **339**, 303–307.
30 Y. Rogan, L. Starannikova, V. Ryzhikh, Y. Yampolskii, P. Bernardo, F. Bazzarelli, J. C. Jansen and N. B. McKeown, *Polym. Chem.*, 2013, **4**, 3813–3820.
31 E. Tocci, L. De Lorenzo, P. Bernardo, G. Clarizia, F. Bazzarelli, N. B. McKeown, M. Carta, R. Malpass-Evans, K. Friess, K. Pilnacek, M. Lanc, Y. P. Yampolskii, L. Strarannikova, V. Shantarovich, M. Mauri and J. C. Jansen, *Macromolecules*, 2014, **47**, 7900–7916.
32 X. H. Ma and I. Pinnau, *Macromolecules*, 2018, **51**, 1069–1076.
33 B. S. Ghanem, R. Swaidan, X. H. Ma, E. Litwiller and I. Pinnau, *Adv. Mater.*, 2014, **26**, 6696–6700.

34 B. S. Ghanem, R. Swaidan, E. Litwiller and I. Pinnau, *Adv. Mater.*, 2014, **26**, 3688–3692.
35 M. Carta, M. Croad, R. Malpass-Evans, J. C. Jansen, P. Bernardo, G. Clarizia, K. Friess, M. Lanc and N. B. McKeown, *Adv. Mater.*, 2014, **26**, 3526–3531.
36 I. Rose, M. Carta, R. Malpass-Evans, M.-C. Ferrari, P. Bernardo, G. Clarizia, J. C. Jansen and N. B. McKeown, *ACS Macro Lett.*, 2015, **4**, 912–915.
37 R. Williams, L. A. Burt, E. Esposito, J. C. Jansen, E. Tocci, C. Rizzuto, M. Lanc, M. Carta and N. B. McKeown, *J. Mater. Chem. A*, 2018, **6**, 5661–5667.
38 R. Swaidan, B. Ghanem and I. Pinnau, *ACS Macro Lett.*, 2015, **4**, 947–951.
39 I. Rose, C. G. Bezzu, M. Carta, B. Comesana-Gandara, E. Lasseuguette, M. C. Ferrari, P. Bernardo, G. Clarizia, A. Fuoco, J. C. Jansen, K. E. Hart, T. P. Liyana-Arachchi, C. M. Colina and N. B. McKeown, *Nat. Mater.*, 2017, **16**, 932–937.
40 A. Fuoco, B. Comesana-Gandara, M. Longo, E. Esposito, M. Monteleone, I. Rose, C. G. Bezzu, M. Carta, N. B. McKeown and J. C. Jansen, *ACS Appl. Mater. Interfaces*, 2018, **10**, 36475–36482.
41 Y. Yin and M. D. Guiver, *Nat. Mater.*, 2017, **16**, 880–881.
42 Y. Hu, M. Shiotsuki, F. Sanda, B. D. Freeman and T. Masuda, *Macromolecules*, 2008, **41**, 8525–8532.
43 C. G. Bezzu, M. Carta, M. C. Ferrari, J. C. Jansen, M. Monteleone, E. Esposito, A. Fuoco, K. Hart, T. P. Liyana-Arachchi, C. M. Colina and N. B. McKeown, *J. Mater. Chem. A*, 2018, **6**, 10507–10514.
44 P. M. Budd, B. S. Ghanem, S. Makhseed, N. B. McKeown, K. J. Msayib and C. E. Tattershall, *Chem. Commun.*, 2004, 230–231.
45 H. Hart, C. Lai, G. C. Nwokogu and S. Shamouilian, *Tetrahedron*, 1987, **43**, 5203–5224.
46 F. Bailly, F. Cottet and M. Schlosser, *Synthesis*, 2005, 791–797, DOI: 10.1055/s-2005-861813.
47 R. S. Luo, J. H. Liao, L. Xie, W. J. Tang and A. S. C. Chan, *Chem. Commun.*, 2013, **49**, 9959–9961.
48 P. M. Budd, N. B. McKeown, B. S. Ghanem, K. J. Msayib, D. Fritsch, L. Starannikova, N. Belov, O. Sanfirova, Y. Yampolskii and V. Shantarovich, *J. Membr. Sci.*, 2008, **325**, 851–860.
49 P. Bernardo, F. Bazzarelli, F. Tasselli, G. Clarizia, C. R. Mason, L. Maynard-Atem, P. M. Budd, M. Lanc, K. Pilnacek, O. Vopicka, K. Friess, D. Fritsch, Y. P. Yampolskii, V. Shantarovich and J. C. Jansen, *Polymer*, 2017, **113**, 283–294.
50 R. Swaidan, B. Ghanem, E. Litwiller and I. Pinnau, *Macromolecules*, 2015, **48**, 6553–6561.
51 L. Starannikova, V. Khodzhaeva and Y. Yampolskii, *J. Membr. Sci.*, 2004, **244**, 183–191.
52 Z. X. Low, P. M. Budd, N. B. McKeown and D. A. Patterson, *Chem. Rev.*, 2018, **118**, 5871–5911.
53 K. D. Dorkenoo and P. H. Pfromm, *Macromolecules*, 2000, **33**, 3747–3751.
54 L. M. Robeson, B. D. Freeman, D. R. Paul and B. W. Rowe, *J. Membr. Sci.*, 2009, **341**, 178–185.
55 V. Teplyakov and P. Meares, *Gas Sep. Purif.*, 1990, **4**, 66–74.
56 R. Swaidan, B. S. Ghanem, E. Litwiller and I. Pinnau, *J. Membr. Sci.*, 2014, **457**, 95–102.
57 J. Wu, J. T. Liu and T. S. Chung, *Adv. Sustainable Syst.*, 2018, **2**, 1800044.
58 N. Du, H. B. Park, G. P. Robertson, M. M. Dal-Cin, T. Visser, L. Scoles and M. D. Guiver, *Nat. Mater.*, 2011, **10**, 372–375.
59 C. R. Mason, L. Maynard-Atem, N. M. Al-Harbi, P. M. Budd, P. Bernardo, F. Bazzarelli, G. Clarizia and J. C. Jansen, *Macromolecules*, 2011, **44**, 6471–6479.
60 J. Zhang, H. Kang, J. Martin, S. Zhang, S. Thomas, T. C. Merkel and J. Jin, *Chem. Commun.*, 2016, **52**, 6553–6556.
61 H. B. Park, C. H. Jung, Y. M. Lee, A. J. Hill, S. J. Pas, S. T. Mudie, E. Van Wagner, B. D. Freeman and D. J. Cookson, *Science*, 2007, **318**, 254–258.